Potential Beneficial Effects of Electron-Hole Plasmas Created in Silicon Sensors by XFEL-Like High Intensity Pulses for Detector Development

Joel T. Weiss[1], Julian Becker[1], Katherine S. Shanks[1], Hugh T. Philipp[1], Mark W. Tate[1] and Sol M. Gruner[1,2,a)]

[1]*Laboratory of Atomic and Solid State Physics, Cornell University, Ithaca, NY 14853, USA*
[2]*Cornell High Energy Synchrotron Source (CHESS), Cornell University, Ithaca, NY 14853, USA*

[a)]Corresponding author: smg26@cornell.edu

Abstract. There is a compelling need for a high frame rate imaging detector with a wide dynamic range, from single x-rays/pixel/pulse to $> 10^6$ x-rays/pixel/pulse, that is capable of operating at both x-ray free electron laser (XFEL) and 3rd generation sources with sustained fluxes of $> 10^{11}$ x-rays/pixel/s [1, 2, 3]. We propose to meet these requirements with the High Dynamic Range Pixel Array Detector (HDR-PAD) by (a) increasing the speed of charge removal strategies [4], (b) increasing integrator range by implementing adaptive gain [5], and (c) exploiting the extended charge collection times of electron-hole pair plasma clouds that form when a sufficiently large number of x-rays are absorbed in a detector sensor in a short period of time [6]. We have developed a measurement platform similar to the one used in [6] to study the effects of high electron-hole densities in silicon sensors using optical lasers to emulate the conditions found at XFELs. Characterizations of the employed tunable wavelength laser with picosecond pulse duration have shown Gaussian focal spots sizes of 6 ± 1 μm rms over the relevant spectrum and 2 to 3 orders of magnitude increase in available intensity compared to previous measurements presented in [6]. Results from measurements on a typical pixelated silicon diode intended for use with the HDR-PAD (150 μm pixel size, 500 μm thick sensor) are presented.

MOTIVATION

Experiments planned for hard x-ray free electron lasers (XFELs) will require detectors with unprecedented dynamic ranges [1, 2, 3]. Several detector efforts, including the adaptive gain integrating pixel detector (AGIPD) and the large pixel detector (LPD), have reported dynamic ranges upwards of 10^5 x-rays per pixel per frame [7, 8]. To push this range further, it may be necessary to use charge removal techniques such as those employed in the Mixed-Mode Pixel Array Detector (MM-PAD) [4].

Pixels relying on a traditional integrating amplifier alone are ultimately limited in full well depth by pixel size, which constrains the size of integration capacitors. The MM-PAD pixels avoid this limitation by pulling a fixed quantity of charge from their front-end when their integrator is nearing saturation and recording the number of charge removals executed in each pixel without interrupting integration. While this strategy has proven immensely useful at storage ring based light sources, the strategy is too slow in its present implementation to keep up with the large signals encountered at XFEL sources.

XFEL pulse durations are on the order of femtoseconds, but the transport properties of silicon diodes employed in most hybrid pixel array detectors slow the entrance of photocurrent into detector pixels significantly. Recent work [6] demonstrated that at particularly high electron-hole pair densities the charge cloud resulting from pulse absorption behaves like a plasma, with the cloud surface screening the diode drift field from the cloud's interior. In this way, the collection of photocurrent from the sensor by a pixel is significantly slowed. Rather than the cloud drifting as a whole, only charge carriers diffusing out of the plasma's central core contribute to photocurrent until the plasma has dissipated. The work presented here seeks to discern how quickly charge removal techniques would need to operate to integrate ultrafast pulses of up to 10^6 x-rays, utilizing this delayed charge collection, so that the High Dynamic Range Pixel Array Detector (HDR-PAD, currently in design phase [9]) can meet these specifications.

METHODS

The transient current technique is utilized to measure the transient photocurrent in a pixel of a hybrid pixel array detector when XFEL-like pulses of up to 10^6 x-rays are incident. A pulsed, tunable-wavelength infrared (IR) laser is used to simulate x-ray pulses. This approach is based on the matching of attenuation lengths in silicon of x-rays and IR photons. For example, the attenuation length in silicon of 1016nm photons matches that of 12 keV x-rays. Table 1 enumerates several x-ray energies along with their attenuation length in silicon and the IR wavelength with the same attenuation length in silicon. In this way, a pulsed IR laser can simulate the electron-hole pair distribution created in silicon sensors upon the absorption of an intense x-ray pulse. The photocurrent produced by IR pulses can then be measured to inform the design of x-ray detectors intended to integrate equivalent x-ray pulses.

We build on previous studies [6], increasing the laser intensity employed by two orders of magnitude, to investigate the delay of photocurrent collection due to the so-called plasma effect. We hope to maximally exploit this mechanism, extending charge collection times of femtosecond XFEL pulses to microseconds. This extended pulse duration may allow for charge removal techniques, perhaps modifications of the technique employed in the MM-PAD, to be used at XFELs.

Data was collected by focusing a tunable, pulsed IR laser (EKSPLA PT259-AO-H) to a $6 \pm 1\mu$m rms spot onto a custom diode modeled after the variety intended for use with the HDR-PAD. The diode is 500μm thick n-type silicon with a 120V depletion voltage and 150μm pixel pitch. Photocurrent transients were terminated with 50Ω on a custom PCB and measured by a Tektronix DPO 7254C oscilloscope. A 1% beam sampling mirror was used with an additional photodiode to measure laser intensity pulse-to-pulse.

RESULTS

Photocurrent transients from XFEL-like pulses have the characteristic shape illustrated in Fig. 1. Focused pulse transients typically arrive at detector pixels as a "spike" followed by a "tail." The tail is a result of the plasma effect, wherein a dense electron-hole pair cloud created in a sensor requires an extended duration to be pulled to collection electrodes due to the screening effect of the cloud. A larger fraction of total charge contributes to the tail when denser electron-hole pair clouds are created. Pulses of lower energy x-rays and higher intensities create denser electron-hole pair clouds. Lower diode bias voltages extend charge collection times further. The charge collection times measured are still significantly shorter than recombination times in silicon. Pulses of $< 10^3$ x-rays are collected completely in

X-ray Energy	Attenuation Length in Silicon	IR Wavelength
2 keV	1.53 μm	547 nm
4 keV	9.68 μm	780 nm
6 keV	30.3 μm	893 nm
8 keV	67.8 μm	950 nm
10 keV	130 μm	992 nm
12 keV	224 μm	1016 nm
14 keV	353 μm	1033 nm
16 keV	521 μm	1046 nm
18 keV	734 μm	1055 nm

TABLE 1. Table listing some x-ray energies, their attenuation length in silicon, and the IR wavelength with a matching attenuation length in room temperature silicon. X-ray attenuation lengths were drawn from the NIST database, and IR photon attenuation lengths were drawn from [10].

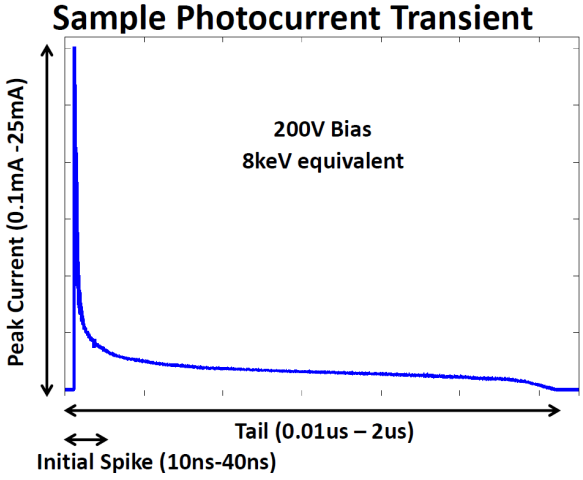

FIGURE 1. Characteristic shape of photocurrent transients produced by high intensity pulses ($> 10^4$ x-rays). The transient above is an average from 950nm pulses (8 keV equivalent attenuation length) with a mean single pulse energy equivalent to 10^6 8keV photons.

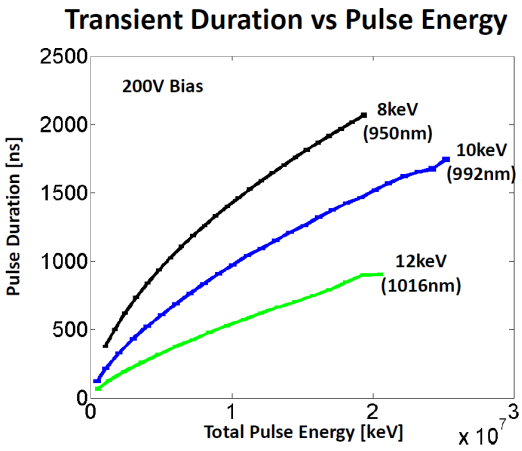

FIGURE 2. Average pulse duration as a function of total pulse energy at three wavelengths. Pulse durations were measured as time above background noise.

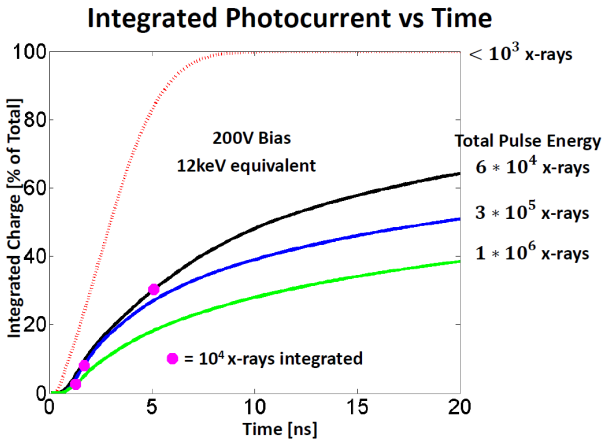

FIGURE 3. Normalized integrated charge versus integration time of 1016 nm (12 keV equivalent attenuation length) pulses at three pulse energies. The red dotted line is a low energy pulse ($< 10^3$ x-rays, simulated from previous work [6]) for reference.

10-40ns, appearing as only a spike, while focused pulses of $> 10^4$ x-rays produce photocurrent tails that can take microseconds to be collected by pixels.

Figure 2 demonstrates how durations of transient tails increase as a function of total pulse energy for three x-ray energy equivalents. Charge collection of 8 keV x-ray equivalent pulses occurs over significantly longer time scales than higher x-ray energy equivalent pulses. This is because the attenuation length of 8 keV x-rays in silicon is significantly shorter than that of 10 keV or 12 keV photons. As a result, charge is deposited in a much smaller volume of the sensor, leading to denser electron-hole pair clouds and therefore more persistent plasma effects. Charge collection times of 12 keV equivalent IR pulses do not reach more than 1µs, but the charge collection times measured are still significantly longer than the laser pulse duration.

This increased charge collection time underpins the strategy of applying charge removal techniques to an x-ray detector intended for use at XFELs. While in-pixel charge removal techniques are not fast enough to act on femtosecond time scales, photocurrent from large pulses may arrive over microseconds, a time period long enough that MM-PAD style charge removal techniques may prove useful. Despite the extended charge collection time, significant photocurrent still arrives in the initial spike.

Figure 3 plots the normalized integral of photocurrent arriving at a pixel versus integration time for three pulse energies with wavelength 1016 nm (12 keV equivalent attenuation length). For reference, the integrated charge versus time of a low intensity pulse ($< 10^3$ x-rays, simulated from previous work [6]) with negligible plasma effects is plotted alongside the data. Integrals are normalized to the total charge integrated by the monitored pixel, which differs from the total charge created by the pulse due to lateral charge spread. Pink dots denote the point at which charge equivalent to 10^4 x-rays has been integrated. Even for a pulse equivalent to only $6x10^4$ 12 keV x-rays, charge equivalent to 10^4 x-rays is integrated within 5 ns of pulse onset. The HDR-PAD will likely feature an adaptive gain front-end, so integrating 10^4 x-rays on timescales faster than charge removal can operate is reasonable. However, very intense pulses of x-rays with energies above 12keV may be problematic. Higher x-ray energy pulses are slowed less by plasma effects and therefore present a worst case scenario to charge removal techniques. Pulses of these wavelengths will have to be characterized further and accounted for in ASIC design goals.

CONCLUSIONS AND FUTURE WORK

An experimental apparatus for utilizing the transient current technique to measure XFEL-like pulses has been constructed and exercised. Pulses with a range of wavelengths and intensities have been measured, and the initial results are illuminating. As expected, the plasma effect is more pronounced for lower x-ray energy equivalents, but still significant at 12 keV. Preliminary results indicate that focused pulses of up to 10^6 x-rays produce photocurrent transients

which are stretched to time scales on which charge removal techniques can conceivably operate.

The data collected and analyzed so far is sufficient to inform testing of the first small scale submission of pixel structures for the HDR-PAD. Inputs to these fabricated pixel front-ends will be modeled after the transients collected in these studies. The results of those tests will inform subsequent HDR-PAD design and laser analysis, but some areas already warrant further investigation.

Significant lateral charge spread has been observed in these studies. The structure of charge clouds and the extent of lateral charge spread is being investigated. Furthermore, incomplete charge collection is observed at low bias voltages (< 160V). Lower bias voltages should extend charge collection times further, but work is needed to find the lowest bias voltage that can reliably collect all deposited charge.

ACKNOWLEDGMENTS

This work is supported by Department of Energy Grant No. DE-FG02-1 0ER46693, NSF award DMR-1332208, and the W.M. Keck Foundation.

REFERENCES

[1] G. Carini, et al., Neutron And X-Ray Detectors, BES Workshop Report (2012). URL: `http://science.energy.gov/~/media/bes/pdf/reports/files/NXD_rpt.pdf`

[2] D. Kramer, et al., Phys. Today 66, (2013). DOI: 10.1063/PT.3.2141

[3] A. Mancuso, et al., Technical Design Report: Scientific Instrument Single Particles, Clusters, and Biomolecules (SPB), (2013). DOI: 10.3204/XFEL.EU/TR-2013-004

[4] M. Tate, et al., J. Phys.: Conf. Ser. 425, (2013). DOI: 10.1088/1742-6596/425/6/062004

[5] H. Graafsma, in Semiconductor Radiation Detection Systems, (CRC Press, 2010), pp. 217-236. ISBN: 978-1-4398-0386-8

[6] J. Becker, Signal Development In Silicon Sensors Used For Radiation Detection, Ph.D thesis, University of Hamburg, 2010. DOI: 10.3204/DESY-THESIS-2010-033

[7] J. Becker, et al., J. Inst. 8, (2013). DOI: 10.1088/1748-0221/8/06/P06007

[8] A. Koch, et al., J. Inst. 8, (2013). DOI: 10.1088/1748-0221/8/11/C11001

[9] K. Shanks, SRI 2015 Conference Proceedings (2015).

[10] M. Green, et al., Sol. Energ. Mat. Sol. C. 92, (2008). DOI: 10.1016/j.solmat.2008.06.009